Biodesign

Purification, crystallization and X-ray diffraction of heparan sulfate bounded human RAGE

Jun bae Park, Youngki Yoo, Belinda Xiang Yu Ong, Juyeon Kim and Hyun-Soo Cho*

Department of Systems Biology and College of Life Science and Biotechnology, Yonsei University, 50 Yonsei-ro, Seodaemun-gu, Seoul 03722, Republic of Korea. *Correspondence: hscho8@yonsei.ac.kr

Receptor for advanced glycation end products (RAGE) is one of the single transmembrane domain containing receptors and causes various inflammatory diseases including diabetes and atherosclerosis. RAGE extracellular domain has three consecutive IgG-like domains (V-C_1-C_2 domain) which interact with various soluble ligands including heparan sulfate or HMGB1. Studies have shown that each ligand induces different oligomeric forms of RAGE which results in a ligand-specific signal transduction. The structure of mouse RAGE bound to heparan sulfate has been previously determined but the electron density map of heparan sulfate was too ambiguous that the exact position of heparin sulfate could not be defined. Furthermore, the complex structure of human RAGE and heparin sulfate still remains elusive. Therefore, to determine the structure, human RAGE was overexpressed using bacterial expression system and crystallized using the sitting drop method in the condition of 0.1 M sodium acetate trihydrate pH 4.6, 8 % (w/v) polyethylene glycol 4,000 at 290 K. The crystal diffracted to 3.6 Å resolution and the space group is C121 with unit cell parameters a= 206.04 Å, b= 68.64 Å, c= 98.73 Å, α= 90.00°, β= 90.62°, γ= 90.00°.

INTRODUCTION

RAGE is a multi-ligand receptor that interacts with advanced glycation end products (AGE), heparan sulfate (HS), S100 proteins, CD11b/Mac1, phosphatidylserine (PS), advanced oxidation protein products (AOPPs), C3a, high mobility group box1 (HMGB1), amyloid β and lipopolysaccharide (LPS), RNA, DNA (Yamamoto and Yamamoto, 2012). In addition, RAGE induces various signaling cascades which include activation of nuclear factor κ-light-chain-enhancer of activated B cells (NF-κB), mitogen-activated protein kinases (MAPKs), phosphoinositiol-3-kinase/protein kinase B (PI3K/Akt), Rho GTPases, Janus kinase/signal transducers and activators of transcription (Jak/STAT) and Sarcoma-family kinases. And some of these signal cascades play a critical role in cancer development, pro-inflammatory gene activation and are related to chronic disorders (Bierhaus et al., 2001). Thus, RAGE has been regarded as a potential target for drug discovery.

The extracellular domain of RAGE consists of three consecutive IgG-like domains (V-C_1-C_2 domain). Research has shown that most of the S100 proteins bind to the V domain except for S100A6 and S100A13, which mainly interact with both the C_1 and C_2 or C_2 domain only, respectively (Yatime et al., 2016) (Rani et al., 2014). It was also found that amyloid β-peptides insoluble aggregates (AβA) interact with the C_1 domain. Hence, it is evident that various RAGE ligands interact specifically with the different RAGE domains.

When RAGE is activated, oligomerization of RAGE occurs and this process has been found to be essential for signal transduction (Dattilo et al., 2007) (Fritz, 2011). In recent years, several structural studies had been carried out to understand the oligomerization of RAGE during RAGE activation. In a particular study conducted by Sirois et al., it was shown that in the DNA bounded RAGE structure, two different RAGE molecules form dimers which are mediated by bound DNA (Sirois et al., 2013). In the structure, the basic pocket of RAGE interacts with the negatively charged DNA through ionic interactions. But, the crystal structure of the heparan sulfate bounded mouse RAGE has been revealed to be a hexamer (Xu et al., 2013). Similar to DNA, heparan sulfate is negatively charged polymer. Hence, it was demonstrated that heparan sulfate also binds to the homo-dimeric V domain pocket of RAGE through ionic interactions. The study also showed that the C_1 domain is first assembled as a homodimer and subsequently as a trimer of dimer (hexamer). Unfortunately, the electron density map of heparan sulfate was too ambiguous to build a model. So, it's not possible to define the exact position of heparan sulfate to demonstrate the atomic interactions between RAGE and heparan sulfate. Therefore, to determine the exact binding mode of heparin sulfate with RAGE, it is necessary to carry out further structural analysis.

RESULTS AND DISCUSSION

Constructed human RAGE (RAGE$_{23-243}$, V-C_1 domain, Figure 1(a)) consists of 221 amino acids. The theoretical molecular weight is 24.2kDa and the isoelectric point is 9.51 (more detailed
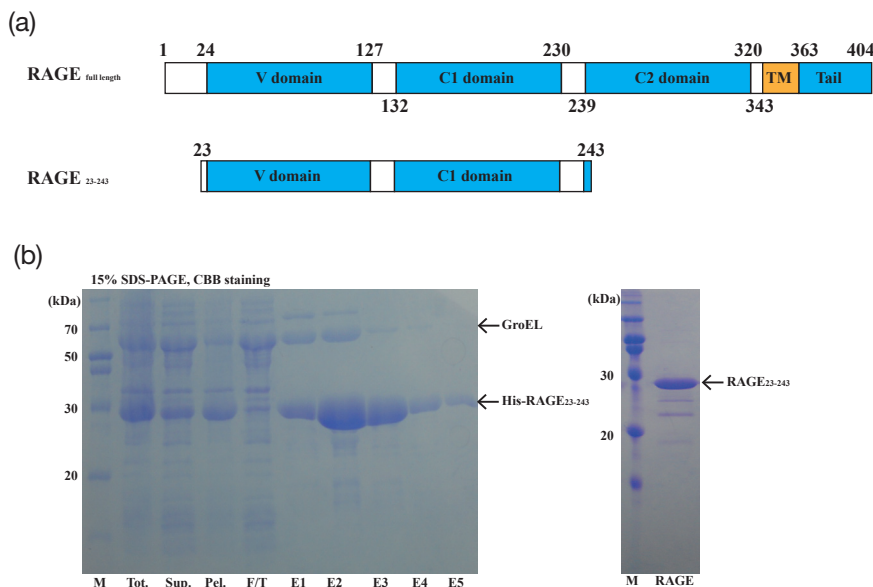
(a)

(b)

FIGURE 1 | **RAGE expression and purification.** (a) Schematic constructed RAGE was expressed as simple stick bar. (b) Confirmation of RAGE$_{23-243}$ overexpression and purification by SDS-PAGE (Left panel). 1 ul of final purified sample was loaded into SDS-PAGE (Right panel). *M: Size marker, Tot: Total cell lysate, Sup: Supernatant of Tot, Pel: Pellet of Tot, F/T: Flow though from nickel bead, E: Elution.

TABLE 1 | RAGE VC$_1$ domain production information

Source organism	Homo sapiens (Human)
DNA source	Synthesized DNA
Uniprot ID	Q15109
Forward primer	CGGAATTCGCTCAAAACATCACAGCCC
Reverse primer	GCCTCGAGTTATGGTTCGATGATGCTGATGC
Cloning vector	modified pET28a
Expression vector	modified pET28a
Expression host	*E.coli* BL21(DE3)pGro7
Complete amino-acid sequence of the construct produced	<u>MGSSHHHHHHSSGLVPRGSHMENLYFQSG</u>SEFAQNITARI GEPLVLKCKGAPKKPPQRLEWKLNTGRTEAWKVLSPQGG GPWDSVARVLPNGSLFLPAVGIQDEGIFRCQAMNRNGKET KSNYRVRVYQIPGKPEIVDSASELTAGVPNKVGTCVSEGSY PAGTLSWHLDGKPLVPNEKGVSVKEQTRRHPETGLFTLQS ELMVTPARGGDPRPTFSCSFSPGLPRHRALRTAPIQPRVWE PVPLEEVQLVVE

*Underline means His tag and TEV protease recognition site.

information of RAGE is described in Table1). Previous studies demonstrated that RAGE$_{23-243}$ contains two disulfide bonds (the V and C$_1$ domain contains a disulfide bond for each) and co-expression of the GroEL chaperone increases the final yield of soluble RAGE. Although more recombinant RAGE appeared in the insoluble fraction than the solution fraction (Figure 1(b) left panel lane3), the total amount of soluble protein was sufficient

for crystal screening. Contaminant GroEL proteins were separated from RAGE by using ion-exchange chromatography and size exclusion chromatography. The purity of the final RAGE$_{23-243}$ sample was further confirmed by SDS-PAGE (Figure 1(b) right panel).

To induce RAGE oligomerization, we used a commercial synthetic heparan sulfate dodecasaccharides (idruron, UK). Through size exclusion chromatography, we confirmed that the synthetic heparan sulfate induces high oligomerization of RAGE. Based on the molecular mass measurement by size exclusion chromatography, the molecular mass of RAGE under ligand-free condition was revealed to be about 5 kDa, unexpectedly. Although the reason for difference in calculated molecular mass is not clear, there might be non-specific interactions between the superdex resin made of polysaccharides and RAGE proteins, which interacts with various materials including DNA, proteins and some polysaccharides. On the other hand, the heparan sulfate bounded RAGE dimer and hexamer were eluted as their expected sizes of 50kDa and 160 kDa respectively (Figure 2).

We collected the fractions of the RAGE peak which corresponds to the hexamer size in the size exclusion chromatography and concentrated the protein to 7 mg/ml. Next, we performed crystallization screening using the Mosquito device (TTP Labtech. USA). The crystal plate was subsequently incubated at 290 K. After five days, it was noted that stick-shaped protein crystal appeared in the 0.1 M sodium acetate trihydrate pH 4.6, 8% (w/v) polyethylene glycol (PEG) 4,000 condition wells (Figure 3(a)). In addition, 15% ethylene glycol was added to the precipitant solution as a cryo-protectant and the crystals were flash frozen in liquid nitrogen. Lastly, the micro-focus beamline (BL-1A) at the photon factory was used for the collection of diffraction data (Tsukuba, Japan).

The heparan sulfate bounded RAGE crystal was diffracted to 3.6 Å resolution (Figure 3(b)). The crystal was grown in space group C121, with unit-cell parameters a= 206.04, b= 68.64, c= 98.73, α= 90.00°, β= 90.62°, γ= 90.00°. To check the effect of
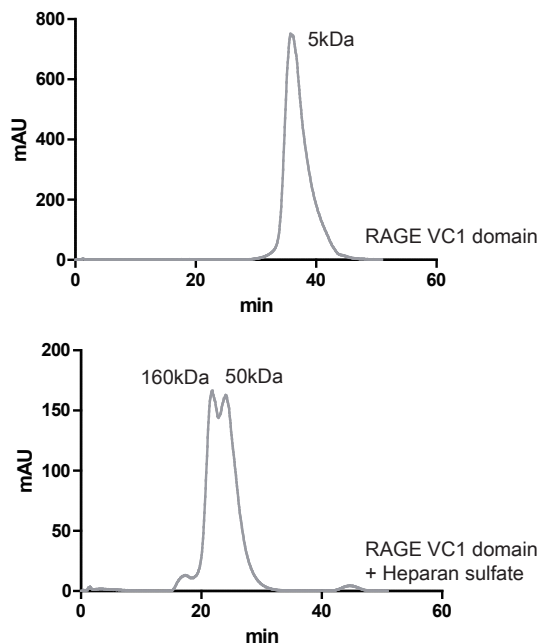
FIGURE 2 ǀ Size exclusion chromatography graphs of ligand-free RAGE VC$_1$ domain and heparan sulfate added RAGE VC$_1$ domain.

TABLE 2 ǀ Data collection and processing

Data collection	
Diffraction source	BL-1A, Photon factory, Japan
Wavelength (Å)	1.1
Temperature (K)	100
Detector	Eiger X4M
Crystal-to-detector distance (mm)	203.8
Rotation range per image (°)	1
Total rotation range (°)	270
Exposure time per image (s)	1
Space group	C121
a, b, c (Å)	206.04, 68.64, 98.73
α, β, γ (°)	90.00, 90.62, 90.00
Resolution range (Å)	54.45-3.60 (3.94-3.60)
Total No. of reflections	16281
Completeness (%)	100 (100)
R$_{merge}$ (%)	12.0 (23.4)
R$_{p.i.m}$ (%)	6.3 (12.1)
I / σI	10.8 (6.4)
Redundancy	4.7 (5.0)

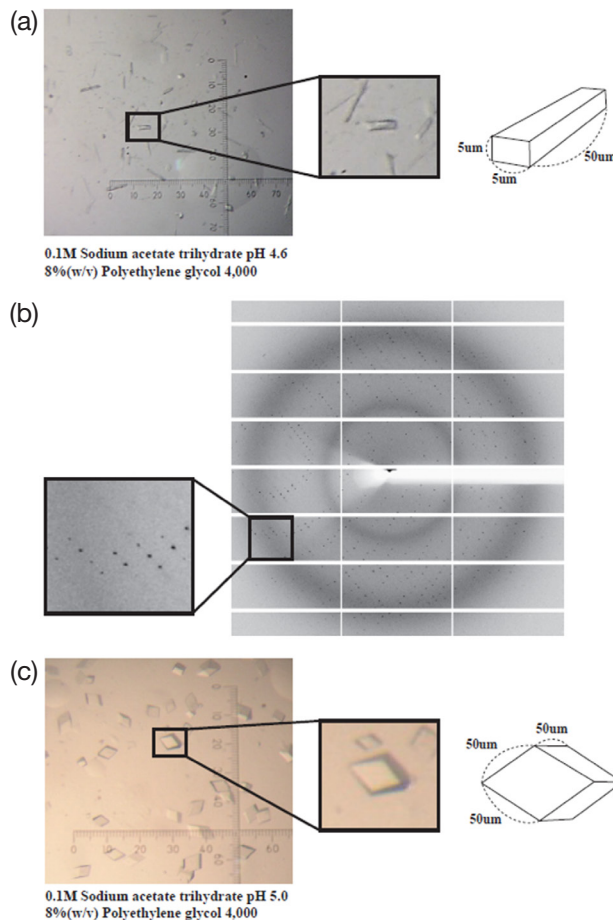*The data for the highest resolution shell is shown in parentheses.

FIGURE 3 ǀ **Heparan sulfate bounded RAGE crystals and X-ray diffraction data.** (a) Stick-shaped crystal under pH 4.6 condition. (b) X-ray diffraction result of crystal (a). (c) Rhombohedral shape crystal under pH 5.0 condition.

pH in crystallization, we attempted to produce crystals under various pH conditions (pH 4.4, pH 4.6, pH 4.8, pH 5.0, pH 5.2) in the same crystal solution. It was found that at pH 4.4, pH 4.6 and pH 4.8, long extended stick-shaped crystals were produced, while rhombohedral shaped crystals appeared at pH 5.0 and pH 5.2 (Figure 3(c)). We also collected the X-ray diffraction data of rhombohedral shaped crystals but the radiation damage was too extensive to collect the full data (Data not shown). The rhombohedral shaped crystal belongs to the R32 space group with unit cell parameter a= 139.56, b= 139.56, c= 280.54, α= 90°, β= 90°, γ= 120°. Based on this data, the packing state of the crystals seems to be different under different pH conditions.

In addition, we calculated the value of Matthew's coefficient to determine the number of RAGE molecules present in the unit cell. As a result, 4 RAGE molecules were possible for rhombohedral crystal. (Matthew's coefficient is 2.72 and solvent percentage is 54.74) And, the stick-shaped crystal is expected to have about 5 molecules. (Matthew's coefficient is 2.88 and solvent percentage is 57.39) In physiological conditions, further studies are needed

Jun bae Park, Youngki Yoo, Belinda Xiang Yu Ong, Juyeon Kim and Hyun-Soo Cho

to determine whether RAGE is functionally regulated by pH condition.

METHODS

Cloning, protein expression and purification of RAGE

The RAGE$_{23-243}$ gene was amplified by PCR from synthesized DNA and cloned into a modified pET28a vector which contains a tobacco etch virus (TEV) protease recognition site (ENLYFQG) between the N-terminal 6xHis and multi-cloning site. The pET28a-RAGE$_{23-243}$ plasmid was inserted into BL21(DE3) pGro7 via transformation and grown in high salt Luria-Broth medium until optical density reaches to 0.6~0.8 at 37°C. The temperature is then decreased to 17°C and over-expression is induced by using 0.3 mM of 1-thio-ß-D-galactopyranoside (IPTG) and 0.2% arabinose for 16 hours. 6xHis-RAGE$_{23-243}$ was purified via metal-affinity chromatography using a Ni-NTA column (GE healthcare) and digested with TEV protease for 16 hours at 4°C. Buffer change was carried out to remove imidazole and to decrease the salt concentration. The desalted protein sample was loaded into a Hitrap-S column (GE Healthcare) and Hiload 26/600 column (GE Healthcare), sequentially. The single and homogeneous RAGE$_{23-243}$ peak fractions were subsequently stored.

Crystallization

Purified RAGE was concentrated using 10 kDa cut-off amicon tube (Merck-Millipore) to 30 mg/ml and HS was added in a molar ratio of 1:2 (2 is HS). The sample was incubated on ice for one hour and subsequently, size exclusion chromatography (Hiload 26/600, GE Healthcare) was performed. The fractions which correspond to the hexamer size of RAGE were collected and concentrated to 7 mg/ml. Next, crystal screening was carried out using the Mosquito device (TTP Labtech, USA). The crystals were grown in a 290 K incubator and after five days, the crystals were observed using a stereomicroscope (SMZ800, Nikon, Japan). Lastly, the crystals were reproduced to a suitable number and size. The optimized crystal was found to be under 0.1 M sodium acetate tri-hydrate pH 4.6, 8 % (w/v) PEG 4,000 condition.

X-ray diffraction

Diffraction data was collected on BL-1A at the photon factory (Tsukuba, Japan) using the Eiger X4M (DECTRIS) detector. For data collection, all crystals were transferred to a cryogenic buffer which is supplemented with 15% ethylene glycol to crystal solution and flash-cooled in liquid nitrogen. Diffraction data was collected at 1.1Å wavelength. The collected data was then integrated and indexed using *iMosflm* (Battye et al., 2011), and scaled using *Aimless* (Evans and Murshudov, 2013) in *CCP4* (Winn et al., 2011) package. More detailed information is described in Table 2.

CONFLICT OF INTEREST

The authors have declared that no competing of interests exists.

ACKNOWLEDGEMENTS

We would like to thank the staff at the Photon Factory beamline 1A

REFERENCES

Battye, T.G., Kontogiannis, L., Johnson, O., Powell, H.R., and Leslie, A.G. (2011). iMOSFLM: a new graphical interface for diffraction-image processing with MOSFLM. *Acta Crystallogr D Biol Crystallogr* **67**, 271-281.

Bierhaus, A., Schiekofer, S., Schwaninger, M., Andrassy, M., Humpert, P.M., Chen, J., Hong, M., Luther, T., Henle, T., Kloting, I., Morcos, M., Hofmann, M., Tritschler, H., Weigle, B., Kasper, M., et al. (2001). Diabetes-associated sustained activation of the transcription factor nuclear factor-kappaB. *Diabetes* **50**, 2792-2808.

Dattilo, B.M., Fritz, G., Leclerc, E., Kooi, C.W., Heizmann, C.W., and Chazin, W.J. (2007). The extracellular region of the receptor for advanced glycation end products is composed of two independent structural units. *Biochemistry* **46**, 6957-6970.

Evans, P.R., and Murshudov, G.N. (2013). How good are my data and what is the resolution? *Acta Crystallogr D Biol Crystallogr* **69**, 1204-1214.

Fritz, G. (2011). RAGE: a single receptor fits multiple ligands. *Trends Biochem Sci* **36**, 625-632.

Rani, S.G., Sepuru, K.M., and Yu, C. (2014). Interaction of S100A13 with C2 domain of receptor for advanced glycation end products (RAGE). *Biochim Biophys Acta* **1844**, 1718-1728.

Sirois, C.M., Jin, T.C., Miller, A.L., Bertheloot, D., Nakamura, H., Horvath, G.L., Mian, A., Jiang, J.S., Schrum, J., Bossaller, L., Pelka, K., Garbi, N., Brewah, Y., Tian, J., Chang, C.S., et al. (2013). RAGE is a nucleic acid receptor that promotes inflammatory responses to DNA. *J Exp Med* **210**, 2447-2463.

Winn, M.D., Ballard, C.C., Cowtan, K.D., Dodson, E.J., Emsley, P., Evans, P.R., Keegan, R.M., Krissinel, E.B., Leslie, A.G., McCoy, A., McNicholas, S.J., Murshudov, G.N., Pannu, N.S., Potterton, E.A., Powell, H.R., et al. (2011). Overview of the CCP4 suite and current developments. *Acta Crystallogr D Biol Crystallogr* **67**, 235-242.

Xu, D., Young, J.H., Krahn, J.M., Song, D., Corbett, K.D., Chazin, W.J., Pedersen, L.C., and Esko, J.D. (2013). Stable RAGE-heparan sulfate complexes are essential for signal transduction. *ACS Chem Biol* **8**, 1611-1620.

Yamamoto, Y., and Yamamoto, H. (2012). Interaction of receptor for advanced glycation end products with advanced oxidation protein products induces podocyte injury. *Kidney Int* **82**, 733-735.

Yatime, L., Betzer, C., Jensen, R.K., Mortensen, S., Jensen, P.H., and Andersen, G.R. (2016). The Structure of the RAGE:S100A6 Complex Reveals a Unique Mode of Homodimerization for S100 Proteins. *Structure* **24**, 2043-2052.